Independent Vector Analysis for SSVEP Signal Enhancement

Darren K. Emge*, François-Benoît Vialatte†, Gérard Dreyfus† and Tülay Adalı*
*Department of CSEE, University of Maryland, Baltimore County, MD 21250
† ESPCI ParisTech, SIGnal processing and MAchine learning (SIGMA) lab,
10, rue Vauquelin, 75231 Paris Cedex 05, France

***Abstract*—Steady state visual evoked potentials (SSVEP) have been identified as a highly viable solution for brain computer interface (BCI) systems. The SSVEP is observed in the scalp-based recordings of electroencephalogram (EEG) signals, and is one component buried amongst the normal brain signals and complex noise. By taking advantage of sample diversity, higher order statistics and statistical dependencies associated with the analysis of multiple datasets, independent vector analysis (IVA) can be used to enhance the detection of the SSVEP signal content. In this paper, we present a novel method for detecting SSVEP signals by treating each EEG signal as a stand alone data set. IVA is used to exploit the correlation across the estimated sources, as well as statistical diversity within datasets to enhance SSVEP detection, offering a significant improvement over averaging based methods for the detection of the SSVEP signal.**

Index Terms— Independent Vector Analysis, Steady-State Visual Evoked Potentials, SSVEP, Brain Computer Interface, BCI

I. Introduction

Brain computer interface (BCI) systems allow for direct connection between a human and a computer, for instance, between a person with severe disabilities and their environment [1]. Steady-state visual evoked potentials (SSVEP) have been identified as one of several signals that can be used for this purpose. The relatively high rate of information transfer and reduced training requirements [2] associated with the SSVEP, make this a highly qualified candidate.

The SSVEP signal is an evoked signal present in the recorded scalp-based electroencephalogram (EEG) when a subject observes a visual stimulus, such as a pattern of flashing lights at a set frequency. The SSVEP will appear in the recorded EEG at the frequency of the visual stimulus and its harmonics [3] mixed with both spontaneous EEG signals associated with normal brain activity as well as complex background noises associated with scalp-based recordings. The central challenge is therefore, to accurately detect and identify the presence of the SSVEP signal, which is critical to the development of a BCI system. To address this challenge, one typical approach for its detection is to take advantage of the phase-locked and stationary nature of the SSVEP and use averaging. Breaking the signal for each individual channel into short time epochs, typically on the order of a few seconds, and averaging [4], the contribution of random and transient signals can be reduced. The average can be Fourier transformed and the SSVEP frequency detected directly, or correlation of the average with a series of pre-constructed sine and cosine references can be used. The use of pre-constructed references, known as source matching, is complicated by the need to shift the reference signals to address misalignment in phase between the average signal and the reference.

We make use of the rich framework of joint blind source separation (JBSS) to take advantage of the sample diversity and higher order statistics to enhance the detection performance for SSVEP. Independent vector analysis (IVA) is an effective solution for performing JBSS for multiple data sets, and is an extension of independent component analysis (ICA) to multiple datasets. IVA has been shown to be an effective solution for capturing independence within individual datasets while preserving the correlation of the source estimates across those data sets [5].

We present a novel approach for analyzing EEG signals to determine the SSVEP content by placing the data into JBSS framework, and applying IVA. This work will show a significant performance enhancement over standard averaging-based techniques in detecting and identifying the SSVEP signal.

II. Methods

Each channel of the EEG signal can be broken into a series of short time epochs, which then as a group, can be treated as a dataset. Using this framework, we can represent each channel as a random vector using superscript notation as $\mathbf{x}^{[k]} = \left[x_1^{[k]}, ..., x_n^{[k]}, ..., x_N^{[k]}\right]^T$, with $k = 1, ..., K$. Assuming that each dataset is a linear mixture of N statistically independent sources, we can take advantage the JBSS framework to detect the SSVEP content. In this application, IVA is of particular interest due to its ability to achieve JBSS based on the sample diversity and higher-order statistics (HOS) within each

978-1-4799-8428-2/15/$31.00 ©2015 IEEE

dataset. Moreover, IVA simultaneously exploits dependencies of the corresponding source estimates across all datasets, making it ideal for multi-set JBSS. Using the generative mixture model, each data set can be written as

$$\mathbf{x}^{[k]} = \mathbf{A}^{[k]}\mathbf{s}^{[k]} \quad k = 1, ..., K \tag{1}$$

where each $\mathbf{A}^{[k]}$ is an N by N mixing matrix, containing the mixing profiles, and $\mathbf{s}^{[k]} = \left[s_1^{[k]}, ..., s_n^{[k]}, ..., s_N^{[k]}\right]^T$ is a random vector representing the signal sources for the kth dataset.

IVA simultaneously estimates the de-mixing matrix $\mathbf{W}^{[k]}$ for each dataset, which results in the source estimates

$$\mathbf{y}^{[k]} = \mathbf{W}^{[k]}\mathbf{x}^{[k]} \quad k = 1, ..., K, \tag{2}$$

where $\mathbf{y}^{[k]} = \left[y_1^{[k]}, ..., y_n^{[k]}, ..., y_N^{[k]}\right]^T$ is a random vector representing the source estimates for the kth dataset. The corresponding source estimates from each dataset can be formed into a source component vector (SCV), one source estimate from each dataset, and is given as $\mathbf{y}_n = \left[y_n^{[1]}, ..., y_n^{[k]}, ..., y_n^{[K]}\right]^T$, $n = 1, ..., N$. The mutual information within each SCV is maximized as part of the IVA cost function which can be written as [6]

$$\mathcal{I}_{\text{IVA}}(\mathcal{W}) = \sum_{n=1}^{N}\left(\sum_{k=1}^{K}\mathcal{H}(y_n^{[k]}) - \mathcal{I}(\mathbf{y}_n)\right) - \sum_{k=1}^{K}\log\left|\det\mathbf{W}^{[\mathbf{k}]}\right| - C \tag{3}$$

where $\mathcal{W}$ is the set of all de-mixing matrices, $\mathbf{W}^{[k]}$ to be estimated, $\mathcal{H}$ is the entropy of the source estimates, $\mathcal{I}$ is the mutual information within an SCV, and C is a constant. IVA thus minimizes the entropy of the individual source estimates, and exploits existing dependencies across data sets by maximizing the mutual information within each SCV, taking all the datasets into account simultaneously. If there is no dependence across datasets the mutual information term $\mathcal{I}(\mathbf{y}_n)$ drops out, and the IVA cost function in (3) becomes equivalent to the ICA cost across each dataset individually

$$\mathcal{I}_{\text{ICA}} = \sum_{n=1}^{N}\sum_{k=1}^{K}\mathcal{H}(y_n^{[k]}) - \sum_{k=1}^{K}\log\left|\det\mathbf{W}^{[\mathbf{k}]}\right| - C \tag{4}$$

If there is only one data set, $K = 1$, it reduces tot the ICA cost written as

$$\mathcal{I}_{\text{ICA}}(\mathbf{W}) = \sum_{n=1}^{N}\mathcal{H}(y_n) - \log|\det(\mathbf{W})| - C.$$

III. Implementation

In this work, we present the analysis of EEG recordings for eight healthy subjects. All participants had normal or corrected to normal vision with no history of migraine, epilepsy or any other neurological disorder. Experimental protocol was explained to all the participants before the experiment. The experiment followed the ethical guidelines of the Helsinki declaration [7], and all subjects filled out a consent form.

Data was recorded at 1.8 kHz sampling rate across 16 channels based upon the 10–20 international system [8]. While the SSVEP signals can be observed in all 16 recorded EEG channels, the strongest SSVEPs are associated with the visual cortex, and therefore only the occipital electrodes O1, Oz, and O2 are examined due to their proximity to this cortex. Each subject performed three repetitions of the experiment, which consisted of observing a reversing checkerboard pattern at a single frequency for 15 seconds. Four frequencies, 5, 10, 20, and 40 Hz, which cover the range of the standard SSVEP problem space, are used in this study.

In order to detect and identify SSVEP content, standard methods leverage both the stationary and phase-locked nature of the SSVEP itself. The recorded signals are broken into short epochs, on the order of a few seconds, and these epochs are averaged to reduce the effect of random and transient content. The averages can be matched to predefined sources, such as sine and cosine waves at the appropriate frequencies. This method known as source matching suffers from phase misalignment between the recorded signal and predefined source [2]. A more direct method consists of taking the Fourier transform of the epoch averages and determining the frequency content directly. This is known as power spectral density analysis (PSDA), and will serve as a baseline for the comparisons in this work rather than source matching, due to the associated phase alignment issues.

Each experiment consisted of 15-seconds of recorded EEG signals. Since averaging methods utilize short time epochs, and the JBSS approach requires sets of data for each channel, a simple division of the each recording into five epochs, each lasting three seconds, evenly divided the data. Based on the models presented in Section II, this results in 5 estimated sources $y_n^{[k]}$, $n = 1, ..., 5$ for each dataset (channel) $\mathbf{x}^{[k]}$, shown in (2)

In order to quantify the presence of the target frequency, F_t, the signal-to-noise ratio at a given frequency, SNR_F is used. The SNR_F introduced in [3] is defined as

$$\text{SNR}_F = \frac{wF(f)}{\sum_{i=s}^{w/2}F(f + i\Delta f) + \sum_{i=s}^{w/2}F(f - i\Delta f)}, \tag{5}$$

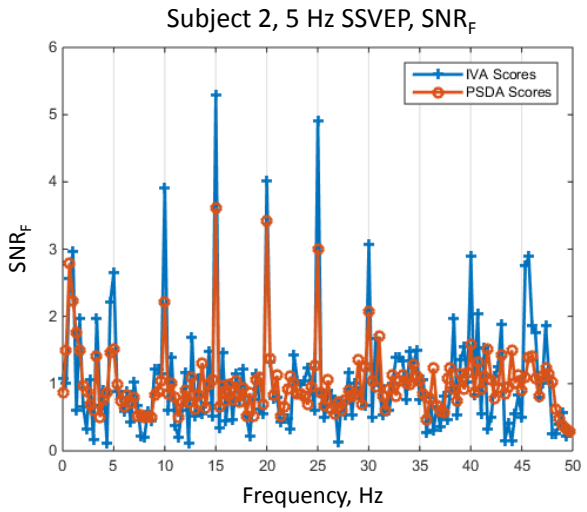

Fig. 1. SNR$_F$ scores for Subject 2, experiment 2, with 5 Hz SSVEP signal. The IVA decomposition method (blue +) shows higher SNR$_F$ as opposed to those for the PSDA method (red o).

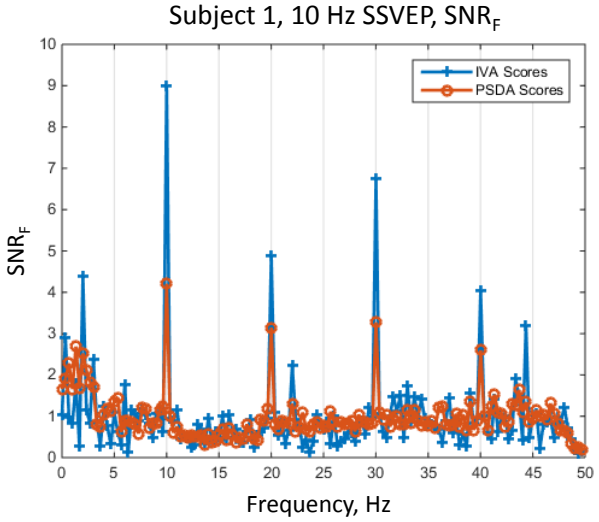

Fig. 2. SNR$_F$ scores for Subject 1, experiment 3, with 10 Hz SSVEP signal. The IVA decomposition method (blue +) shows higher SNR$_F$ as opposed to those for the PSDA method (red o).

where f is frequency, F is the energy of the signal at f, Δf is the frequency step size, and w is the window width. The ideal window is determined through experimentation by varying its symmetrical width. The best choice for this application, proved to be the next lower integer, in terms of sample size, than the number of samples to the closest harmonic of the target SSVEP.

The SNR$_F$ of the PSDA is directly compared to the maximum SNR$_F$ of the five estimated sources using IVA for the Oz channel. The other occipital channels show similar results, however some subjects exhibited unilateral topography, where one side of the cortex had significantly lower enhancement. This would reduce the averaged SNR$_F$ for these subjects, thus biasing the results. Therefore, only the Oz channel SNR$_F$ was used due to its consistency across all subjects.

IV. Results

Using the JBSS framework, explained in Section III, in this section we show that IVA can enhance the detection of the SSVEP by taking advantage of the diversity within each dataset, while simultaneously preserving dependence between corresponding source estimates across datasets. Performance is quantified using the SNR$_F$ and statistically significant improvements are demonstrated using a two sample t-test.

The SNR$_F$ for the lowest frequency, 5 Hz SSVEP is shown in Figure 1 for Subject 2, experiment 2. The SNR$_F$ for the maximum IVA estimated source is shown in blue (+) and the PSDA in red (o). Figure 1 shows an SNR$_F$ of 1.5 for PSDA and 2.6 for IVA, in many instances is it difficult to detect the SSVEP due to the abundance of noise in this region (note the

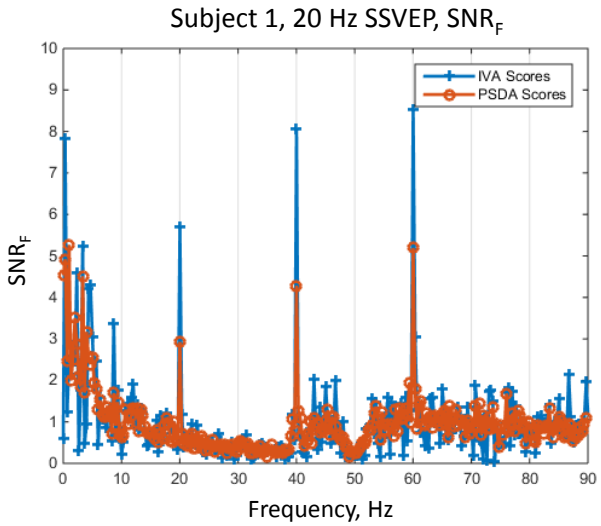

Fig. 3. SNR$_F$ scores for Subject 1, experiment 2, with 20 Hz SSVEP signal. The IVA decomposition method (blue +) shows superior performance to the PSDA method (red o).

increased SNR$_F$ scores at frequencies less than 5 Hz). For frequencies less than 8 Hz, the harmonics are often used to assist in detecting the SSVEP, and Figure 1 shows an average increase of SNR$_F$ for IVA over to PSDA of 1.5 for at all harmonics (H$_i$), $i = 1...6$, where H$_1$ $= f$, H$_i$ $= i \times f$, and f is the SSVEP frequency. Additionally, in the region of the harmonics the noise levels appear to be much lower.

The SSVEP frequency of 10 Hz, is shown in Figure 2. A more pronounced difference for IVA, SNR$_F$ = 9.0,

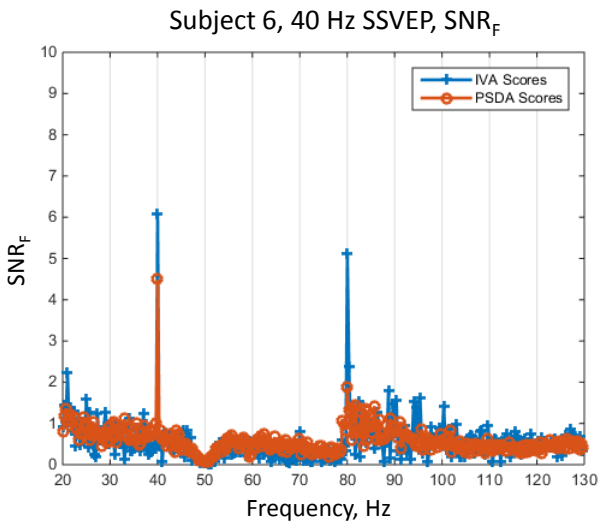

Fig. 4. SNR_F scores for Subject 6, experiment 3, with 40 Hz SSVEP signal. The IVA decomposition method (blue +) shows superior performance to the PSDA method (red o).

over PSDA, SNR_F = 4.2 for Subject 1, experiment 3 is shown. The SNR_F ratio for the primary (IVA/PSDA) is 2.1 which is roughly equivalent to that shown for the odd harmonic ($H_3 = 30$ Hz) which is 2.0. The even harmonics ($H_2 = 20$ and $H_4 = 40$ Hz) show ratios of 1.6 and 1.5 respectively. The relationship across even and odd harmonics has been observed in SSVEP analysis for multiple subjects, but has not proved robust across all subjects.

The 20 Hz SSVEP signal should be relatively easy to detect for both methods used. Figure 3 shows the SNR_F scores for a 20 Hz SSVEP for Subject 1, experiment 2. The IVA continues show increased SNR_F for the primary with an IVA/PSDA ratio of 2.0. The harmonics show an increase as well but the ratios are slightly smaller with the average increase of 1.8 for IVA over PSDA.

At the upper extreme of the frequency range, the 40 Hz SSVEP for Subject 6, experiment 3, is shown in Figure 4. Once again, we see an increase in the IVA over the PSDA, in this case the ratio is 1.3. Only one harmonic is observed at $H_2 = 80$ with a significant increase of 2.7, for IVA over PSDA. This harmonic is of interest and will be addressed further in Section V.

In order for IVA to be useful, it must be robust across the population of subjects. This is demonstrated in Figure 5 for the 5 Hz SSVEP, with each sub-figure showing the SNR_F for all eight subjects at a single harmonic. The eight vertical dotted lines serve to group the three experimental repetitions conducted by each subject, for a total of 24 comparisons. In sub-figure 5(a), we see a 1.5 to 2 times increase in the SNR_F scores for IVA

TABLE I
Statistical analysis of SNR_F score improvements for IVA analysis versus PSDA. The H_1 is the fundamental or target frequency and H_2 is the 2nd harmonic, and H_3 is the third (e.g., 5 Hz SSVEP H_1 =5 Hz, H_2 =10 Hz, and H_3 =15 Hz). There was no obvious signal present for the 3rd harmonic of the 40 Hz target.

SSVEP Target (Hz)	p-value		
	H_1	H_2	H_3
5	3.43×10^{-6}	6.98×10^{-8}	2.21×10^{-11}
10	5.41×10^{-8}	5.11×10^{-7}	1.72×10^{-6}
20	1.67×10^{-8}	1.74×10^{-7}	2.67×10^{-7}
40	8.84×10^{-8}	1.43×10^{-8}	NA

over PSDA for all subjects. The second harmonic at 10 Hz, shown in Figure 5(b), shows a similar increase to that seen in Figure 5(a). Figures 5(c) and 5(d) show the third ($H_3 = 15$ Hz) and fourth ($H_4 = 20$ Hz) harmonics respectively. As the frequency of the harmonic increases the SNR_F for IVA continues to show an increase over PSDA and the variation across subjects tends to decrease. This supports the use of higher harmonics in detecting low frequency SSVEP content. Variation by subject is observed, with the extremes in Subject 4, but the general increase in SNR_F is observed for all subjects.

As the SSVEP target frequency increases from 5 to 40 Hz, an increase in SNR_F is evident at the primary frequency and its harmonics. However, the number of harmonics that appear drops off as the frequency increases. For 5 Hz in Figure 1 five additional harmonics are clearly observed. In Figure 2, this drops to 3 and continues to decrease as the SSVEP frequency increases, and at 40 Hz only one harmonic is observed, as shown in Figure 4. From the data presented, there appears to be an upper limit to the detectable SSVEP harmonics at around 80 Hz.

Statistical quantification is shown using the two sample t-test on the SNR_F scores at the primary frequencies and the first two harmonics. The resulting p-values are shown in Table 1, where the left column shows the target SSVEP frequency, and the associated p-value given for the primary target frequency (H_1), the second harmonic (H_2), and the third harmonic (H_3) are found in the right columns. For all frequencies and corresponding harmonics, the p-values show a significant difference, increase, for IVA over PSDA. Of interest, is the significance of the 5 Hz SSVEP harmonics over the primary frequency, where the second (H_2) and third (H_3) harmonics are more significant. This supports the observation stated above that higher harmonics are often used to assist in detecting the SSVEP at frequencies less than 8 Hz. As shown in Figures 1, 2, and 3 the noise level below 8 Hz is normally higher than that in the higher frequency ranges.

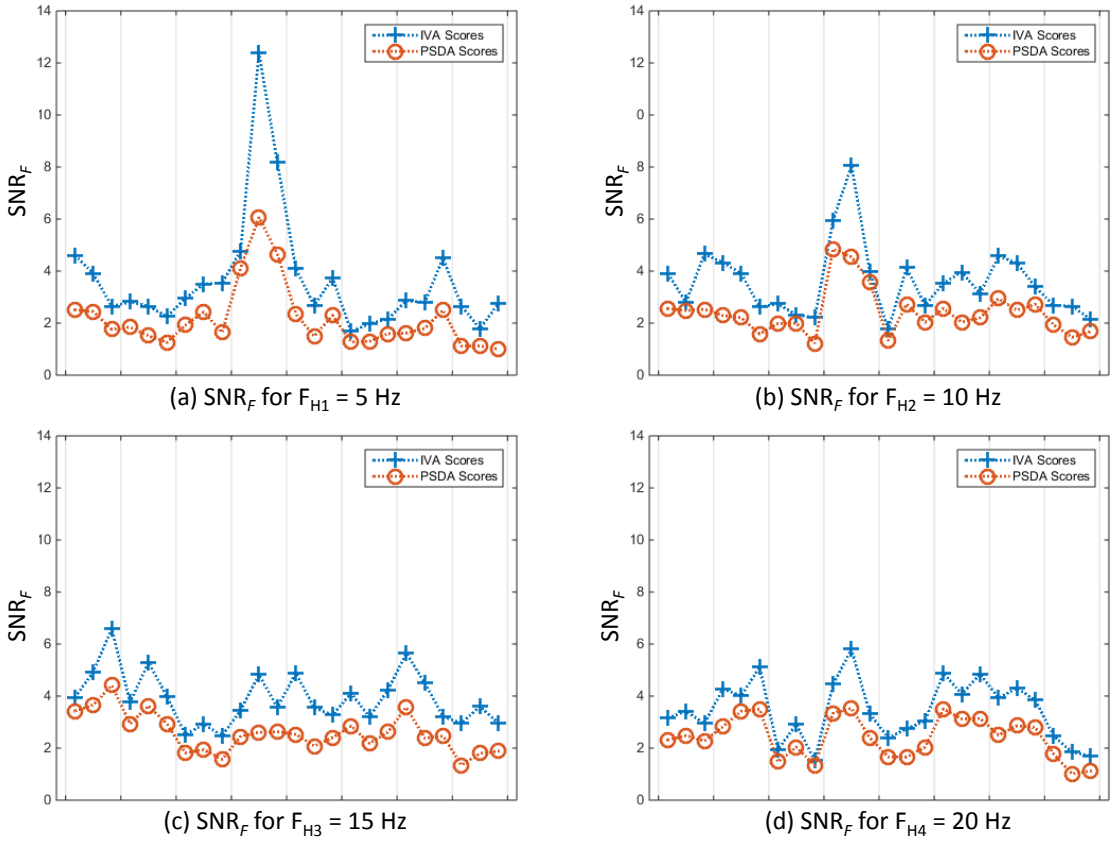

Fig. 5. SNR$_F$ scores for all subjects, all experiments, for the 5 Hz SSVEP target frequency. Vertical bars separate individual subjects, with three SNR$_F$ per subject. Sub-figure (a) shows the scores for the primary or target frequency, $H_1 = 5$ Hz, (b) the second harmonic $H_2 = 10$ Hz, (b) the third harmonic $H_3 = 15$ Hz, and the (b) the fourth harmonic $H_4 = 20$ Hz. At all harmonics, H_i $i = 1, 2, 3, 4$, the IVA decomposition method (blue +) achieves higher SNR$_F$ then that achieved using PSDA (red o).

V. Conclusion

In general, one can observe from the results that using IVA enhances the SSVEP responses across a range of frequencies. This approach has the potential to open new avenues of SSVEP research for both BCI applications and neurocognitive investigations. For example, extending this approach to autonomous de-noising of the EEG data will allow for more general BCI applications. The use of source estimates across subjects could allow for cross subject information to be used in calibration of BCI systems for new users.

Beyond the initial application to BCI, the investigation of scalp topography based on the estimated sources containing SSVEP would be a promising tool in enhancing topographical probes, by providing insights into the SSVEP propagation mechanisms. The Gamma range (above 20 Hz) is of great interest as well for the investigation of cognitive mechanisms [9] and can be used to tag brain response topographies as they relate to visual tasks [10]. These potentials are shown to be useful in monitoring neural correlates of cognitive functions: for instance attention [11] or executive functions [12]. However, the poor signal-to-noise ratio in higher EEG ranges has made results obtained at frequencies above 25 Hz questionable. Figure 4 shows not only the 40 Hz response enhancement but also the high Gamma range harmonic at 80 Hz. This shows that the presented method could extend the limits of EEG investigations, allowing the use of SSVEP for topographic probe investigations of cognitive mechanisms.

VI. Summary

Previous efforts to enhance the SSVEP response have used blind source separation [13], e.g., through manual rejection of ICA sources identified as artifacts for de-noising. In this work, we have presented a method that is autonomous, simple to apply, and can be applied across subjects to enhance the detection of the SSVEP. The use of a JBSS framework is shown to be highly effective for using the sample diversity and higher-order

statistics within channels while leveraging dependence of source estimates across channels to enhance the detection of the SSVEP and its harmonics. The demonstrated enhancements are seen across a range of frequencies and have been shown to be robust across a population of subjects.

VII. Acknowledgment

The authors would like to thank Mr. Antoine Gaume† for designing the experiment and collecting the data used in this work.

References

[1] J. R. Wolpaw, N. Birbaumer, D. J. McFarland, G. Pfurtscheller, and T. M. Vaughan, "Brain–computer interfaces for communication and control," *Clinical neurophysiology*, vol. 113, no. 6, pp. 767–791, 2002.

[2] Y. Zhang, G. Zhou, J. Jin, M. Wang, and A. Cichocki, "L1-regularization multiway cannonical correlation analysis for ssvep-based bci," *IEEE Transactions on Neural Systems and Rehabilitaion Engineering*, vol. 21, no. 6, pp. 887–896, November 2014.

[3] F.-B. Vialatte, M. Maurice, J. Dauwels, and A. Cichocki, "Steady-state visually evoked potentials: Focus on essential paradigms and future perspectives," *Progress in Neurobiology*, vol. 90, no. 4, pp. 418–438, April 2010.

[4] G. R. Müller-Putz, R. Scherer, C. Brauneis, and G. Pfurtscheller, "Steady-state visual evoked potential (ssvep)-based communication: impact of harmonic frequency components," *Journal of neural engineering*, vol. 2, no. 4, p. 123, 2005.

[5] T. Adali, M. Anderson, and G. Fu, "Diversity in independent component and vector analyses: Identifiability, algorithms, and applications in medical imaging," *Signal Processing Magazine, IEEE*, vol. 31, no. 3, pp. 18–33, 2014.

[6] M. Anderson, T. Adali, and X.-L. Li, "Joint blind source separation with multivariate gaussian model: algorithms and performance analysis," *Signal Processing, IEEE Transactions on*, vol. 60, no. 4, pp. 1672–1683, 2012.

[7] W. M. Association *et al.*, "World medical association declaration of helsinki: ethical principles for medical research involving human subjects." *JAMA*, vol. 310, no. 20, p. 2191, 2013.

[8] G. H. Klem, H. O. Lüders, H. Jasper, and C. Elger, "The ten-twenty electrode system of the international federation," *Electroencephalogr Clin Neurophysiol*, vol. 52, no. suppl., p. 3, 1999.

[9] F. Varela, J.-P. Lachaux, E. Rodriguez, and J. Martinerie, "The brainweb: phase synchronization and large-scale integration," *Nature reviews neuroscience*, vol. 2, no. 4, pp. 229–239, 2001.

[10] R. B. Silberstein, *Steady state visually evoked potentials, brain resonances and cognitive processes*, P. L. Nunez, Ed. New York: Oxford University Press, 1995.

[11] D. Kim, G. Wylie, R. Pasternak, P. D. Butler, and D. C. Javitt, "Magnocellular contributions to impaired motion processing in schizophrenia," *Schizophrenia research*, vol. 82, no. 1, pp. 1–8, 2006.

[12] R. B. Silberstein, F. Danieli, and P. L. Nunez, "Fronto-parietal evoked potential synchronization is increased during mental rotation," *NeuroReport*, vol. 14, no. 1, pp. 67–71, 2003.

[13] F.-B. Vialatte, M. Maurice, T. Tanaka, Y. Yamaguchi, and A. Cichocki, "Analyzing steady state visual evoked potentials using blind source separation," in *Proceedings of the Second APSIPA Annual Summit and Conference. Singapore*, 2010, pp. 578–582.